HHS Public Access

Author manuscript

Sci Signal. Author manuscript; available in PMC 2016 February 25.

Published in final edited form as:

Sci Signal. ; 8(391): ra84. doi:10.1126/scisignal.aaa9953.

The G protein α-subunit variant XLαs promotes $G_{q/11}$-dependent signaling and mediates the renal actions of parathyroid hormone in vivo*

Qing He[1], **Yan Zhu**[1], **Braden A. Corbin**[1], **Antonius Plagge**[2], and **Murat Bastepe**[1,*]

[1]Endocrine Unit, Department of Medicine, Massachusetts General Hospital and Harvard Medical School, Boston, MA 02114, USA.

[2]Department of Cellular and Molecular Physiology, Institute of Translational Medicine University of Liverpool, Liverpool, L69 3BX, UK.

Abstract

GNAS, which encodes the stimulatory G protein α subunit (Gαs), also encodes a large variant of Gαs termed XLαs, and alterations in XLαs abundance or activity are implicated in various human disorders. Although XLαs, like Gαs, stimulates generation of the second messenger cAMP, evidence suggests that XLαs and Gαs have opposing effects in vivo. We investigated the role of XLαs in mediating signaling by parathyroid hormone (PTH), which activates a GPCR that stimulates both Gαs and Gαq/11 in renal proximal tubules to maintain phosphate and vitamin D homeostasis. At postnatal day 2 (P2), XLαs-knockout (XLKO) mice exhibited hyperphosphatemia, hypocalcemia, and increased serum concentrations of PTH and 1,25-dihydroxyvitamin D, indicative of compromised PTH responsiveness. The ability of PTH to reduce serum phosphate concentrations was impaired and the abundance of the sodium-phosphate cotransporter Npt2a in renal brush-border membranes was reduced in XLKO mice, whereas PTH-induced cAMP excretion in the urine was modestly increased. Basal and PTH-stimulated production of inositol trisphosphate (IP_3), which is the second messenger produced by Gαq/11 signaling, were repressed in renal proximal tubules from XLKO mice. Crossing of XLKO mice with mice overexpressing XLαs specifically in renal proximal tubules rescued the phenotype of the XLKO mice. Overexpression of XLαs in HEK 293 cells enhanced $G_{q/11}$-dependent signaling

---

*Corresponding author. E-mail: bastepe@helix.mgh.harvard.edu.

SUPPLEMENTARY MATERIALS

Fig. S1. XLαs is located in the kidney at early postnatal stages and XLKO mice do not have defects in renal structure.
Fig. S2. The abundances of Npt2a protein and *Slc20a2* mRNA are similar between P2 WT and XLKO mice.
Fig. S3. Increased renal Gαs abundance in P2 XLKO kidneys.
Fig. S4. The abundances of PKC-βII, PKC-θ, phosphorylated ERK1/2, and phosphorylated substrates of PKA are not decreased in the proximal tubules of P2 XLKO mice.
Table. S1. Sequences of the primer pairs used in qRT-PCR assays.

Competing interests: The authors declare that they have no competing interests.

Author contributions: Q.H., Y.Z., and M.B. conceived and designed the study and wrote the manuscript with input from all the authors; Q.H. performed most of the experiments; Y.Z. and B.A.C assisted in the biochemical measurements; and A.P. provided the XLKO mice and assisted in the interpretation of results.

in unstimulated cells and in cells stimulated with PTH or thrombin, which is a $G_{q/11}$-coupled receptor. Together, our findings suggest that XLαs enhances $G_{q/11}$ signaling to mediate the renal actions of PTH during early postnatal development.

INTRODUCTION

The α-subunit of the stimulatory heterotrimeric guanine nucleotide–binding protein (G_s) mediates the actions of many hormones, neurotransmitters, and autocrine or paracrine factors by stimulating the generation of the second messenger cyclic adenosine monophosphate (cAMP) (1-3). Gαs is encoded by the imprinted *GNAS* complex locus, mutations in which cause multiple genetic diseases with complex parent-of-origin–specific phenotypes. Furthermore, somatic mutations in *GNAS* that lead to constitutive Gαs activity or increased *GNAS* copy number are found in multiple benign and malignant tumors. In addition to Gαs, *GNAS* gives rise to several different gene products, including a variant of Gαs termed extra-large α-subunit (XLαs) (4). XLαs has a distinct N-terminal domain, but is otherwise identical to Gαs. Gαs is expressed biallelically in most tissues; however, paternal Gαs expression is silenced in some tissues, such as certain parts of the brain, thyroid, pituitary gland, and renal proximal tubules (5). In contrast, the XLαs promoter is silenced on the maternal allele and activates transcription exclusively from the paternal allele (6, 7). Thus, most inactivating and all activating *GNAS* mutations affect the expression and activity of XLαs when located on the paternal allele.

In mice and humans, loss of function of XLαs is implicated in intrauterine and perinatal growth retardation, as well as poor adaption to feeding, hypoglycemia, and disrupted glucose counter-regulation (8-11). Epigenetic silencing of XLαs is found in patients with a platelet abnormality characterized by deficient activation of the G_s-cAMP signaling pathway, whereas its overexpression is postulated to contribute to the development of chromosome 20q– amplified breast cancers (12, 13). Loss of imprinting at the *XLαs* promoter in mice, which leads to increased abundance of *XLαs* mRNA, also leads to early postnatal hypoglycemia and lethality (14). Despite the clear importance of this protein in multiple systems, the cellular functions of XLαs itself and relative to the functions of Gαs remain currently unclear. At the biochemical level, XLαs behaves similarly to Gαs and it stimulates G protein–coupled receptor (GPCR)–activated generation of cAMP when it is increased in abundance (15, 16). On the other hand, comparison of the phenotypes of XLαs knockout mice with those of Gαs knockout mice suggests that the two proteins play opposing roles in vivo, and that XLαs has actions that are distinct from those of Gαs (9, 17). Moreover, XLαs has several splice variants and alternative translation products (6, 18-21), which are also ablated or overexpressed upon genetic or epigenetic defects that alter XLαs expression. The relative contributions of XLαs and these other variants to physiology and disease pathogenesis have also remained largely unclear.

To examine the cellular roles of XLαs, we focused on the actions of parathyroid hormone (PTH), which acts through Gαs in the renal proximal tubule to inhibit phosphate reabsorption and to stimulate the synthesis of the bioactive form of vitamin D (22). PTH also uses the $G_{q/11}$ signaling pathway to inhibit phosphate reabsorption in the proximal

tubule, thus stimulating phospholipase Cβ and thereby generating the second messengers inositol 1,4,5-trisphosphate (IP_3) and diacylglycerol (DAG), which is followed by the activation of certain protein kinase C (PKC) isozymes (23). Overexpression studies have also shown that PTH acts through XLαs to stimulate cAMP generation (24). Because XLαs is found in the kidney (16, 24, 25), we investigated whether this imprinted *GNAS* product mediated the actions of PTH in vivo and whether its effects occurred through cAMP signaling. Our investigations showed that the loss of XLαs in the renal proximal tubule disrupted PTH-mediated phosphate handling during early postnatal development and, instead of reducing the generation of cAMP, it led to decreased $G_{q/11}$ signaling. Our additional studies revealed that XLαs promoted basal and agonist-stimulated $G_{q/11}$ signaling in transfected cells and in transgenic mice. Thus, XLαs mediates the proximal tubular actions of PTH and serves as a G protein α-subunit for both G_s and $G_{q/11}$-dependent signaling.

RESULTS

XLαs is located in renal proximal tubule cells during the early postnatal development of mice

XLαs protein is found in whole mouse kidneys in readily detectable amounts at postnatal day 2 (P2), but not P6 (25). Through immunostaining with an XLαs-specific antiserum, we showed that XLαs protein was located in the renal proximal tubules of P2 wild-type mice and, albeit less abundantly, in distal tubules, whereas no immunostaining was detected in other parts of the kidney (Fig. 1, A and B). XLαs protein was undetectable in samples from mice in which the paternal XLαs allele was disrupted (XLKO mice) (Fig. 1, A and B and fig. S1A). Loss of detectable XLαs protein upon ablation of the paternal allele alone is consistent with the exclusively paternal expression of this *GNAS* product, as described previously (6). Because *XLαs* mRNA abundance was greater at P2 than at later times (fig. S1B), we focused our efforts on determining the role of XLαs at P2. Histological analysis detected no obvious defects in tubule structures in P2 XLKO mice, although the kidneys from these mice were smaller compared to those from their wild-type littermates, consistent with the overall smaller size of the XLKO pups (fig. S1C) (9). Nevertheless, the abundance of mRNA for *Kid1*, which encodes a renal transcription factor whose mRNA accumulates in the course of postnatal renal development, was decreased by about 50% in whole kidneys from P2 XLKO mice compared to that in kidneys from wild-type mice, which suggests that there was a delay in proximal tubule development (fig. S1D).

XLKO mice exhibit hyperphosphatemia and hypocalcemia together with increased serum PTH

At the renal proximal tubule, PTH inhibits the reabsorption of inorganic phosphate from the glomerular filtrate and stimulates the synthesis of the active vitamin D metabolite 1,25 dihydroxyvitamin D [$1,25(OH)_2D$], which increases calcium absorption in the small intestine. P2 XLKO pups showed substantially increased concentrations of serum phosphate (hyperphosphatemia), decreased concentrations of serum calcium (hypocalcemia), as well as increased concentrations of serum PTH compared to wild-type mice (Table 1). However, the concentration of $1,25(OH)_2D$ in the serum was also markedly increased, whereas the serum

concentration of fibroblast growth factor 23 (FGF23), another phosphaturic hormone that suppresses $1,25(OH)_2D$ synthesis in the proximal tubule (26), was substantially reduced in abundance in P2 XLKO pups (Table 1).

We then examined the abundance of mRNA for renal 25-hydroxyvitamin D 1α-hydroxylase (*Cyp27b1*), which synthesizes $1,25(OH)_2D$, as well as that of 25-hydroxyvitamin D 24-hydroxylase (*Cyp24a1*), which metabolizes $1,25(OH)_2D$. The abundance of *Cyp27b1* mRNA was increased >5-fold in P2 XLKO kidneys compared to that in P2 wild-type kidneys (Fig. 2A), whereas that of *Cyp24a1* mRNA was moderately increased in P2 XLKO kidneys (Fig. 2B), suggesting that the increased $1,25(OH)_2D$ abundance resulted from induced expression of *Cyp27b1*. We then examined the type II sodium-dependent phosphate cotransporter Npt2a in the renal brush border membrane because of its critical role in the reabsorption of phosphate, and we found that the abundances of its mRNA and protein in P2 XLKO mice were markedly increased compared to those in P2 wild-type mice (Fig 2, C and D). In contrast, the abundances of Npt2c protein and *Slc20A2* (*Pit2*) mRNA, which encodes another sodium-dependent phosphate transporter, were similar in renal brush border membranes from XLKO and wild-type mice, as determined by Western blotting and quantitative reverse transcription polymerase chain reaction (qRT-PCR) analysis, respectively (fig. S2, A to C).

XLKO mice are resistant to PTH despite exhibiting increased excretion of urinary cAMP

PTH stimulates the expression of *Cyp27b1* by acting on its promoter region (27). As expected, two hours after they were injected subcutaneously (s.c.) with PTH (50 nmol/kg), wild-type mice exhibited a ten-fold increase in the abundance of *Cyp27b1* mRNA in their kidneys compared to that in the kidneys of wild-type mice injected with vehicle (Fig. 3A). In contrast the abundance of *Cyp27b1* mRNA was increased by only 1.421-fold in XLKO mice injected with PTH compared to that in vehicle-treated XLKO mice (Fig. 3A). Note that the XLKO pups had much higher basal *Cyp27b1* expression than did wild-type pups (Fig. 3A). PTH stimulates renal phosphate excretion by decreasing the abundance of Npt2a protein in renal brush border membranes and thus leads to hypophosphatemia (28). After they were injected with PTH, P2 wild-type mice had statistically significantly reduced serum phosphate concentrations compared to those in vehicle-treated wild-type mice, whereas the serum phosphate concentration of PTH-treated XLKO mice was not substantially reduced compared to that in vehicle-treated XLKO mice (Fig. 3B). Similarly divergent effects of PTH on renal Npt2a abundance in wild-type and XLKO mice were also observed (Fig. 3, C and D). Fifteen minutes after they were injected with PTH, wild-type mice showed an 80% decrease in the abundance of Npt2a in the renal brush border membrane compared to that in vehicle-treated wild-type mice, whereas the effect of PTH on reducing Npt2a abundance in the renal brush border membranes of XLKO mice was less substantial (Fig. 3, C to E). These results suggest that the proximal tubular actions of PTH in XLKO mice were blunted compared to those in wild-type mice.

To characterize the role of XLαs in mediating the actions of PTH, we tested whether XLKO exhibited a reduction in the PTH-induced secretion of cAMP from the kidney into the urine; a test that is used to assess the proximal tubular action of PTH and to establish a diagnosis of

PTH resistance in patients (29). The basal concentrations of urinary cAMP in P2 wild-type and XLKO mice were similar 15 min after they received s.c. injections of vehicle (Fig. 4A). Injection with PTH led to increased concentrations of urinary cAMP in wild-type and XLKO pups; however, the concentrations were statistically significantly greater in the XLKO mice than in their wild-type littermates (Fig. 4A). We then measured *Gαs* mRNA abundance in whole kidneys and found a moderate, but statistically significant, increase in those of P2 XLKO mice compared to those of wild-type mice (Fig. 4B). Western blotting analysis revealed a three-fold increase in the abundance of Gαs protein in the brush border membranes of XLKO mice compared to that in the brush border membranes of wild-type mice (Fig. 4, C and D). Immunostaining of kidney sections with anti-serum directed against the unique N-terminal portion of Gαs (and that cannot recognize XLαs) was also suggestive of increased amounts of Gαs protein in the kidneys of XLKO mice (fig. S3).

XLKO pups show repressed $G_{q/11}$ signaling

Because the PTH-stimulated generation of cAMP was not impaired in P2 XLKO mice, we examined the $G_{q/11}$ signaling pathway, which can be activated by PTH and contributes to the regulation of serum phosphate concentrations (23, 30, 31). In proximal tubule–enriched renal cortices isolated from P2 XLKO kidneys, we found that the intracellular amount of the IP_3 metabolite inositol monophosphate (IP_1), which reflects IP_3 generation, was substantially reduced under basal conditions, as well as upon stimulation with PTH (Fig. 5A). Western blotting analysis showed that the abundances of PKCδ, PKCα, and PKCζ, but not PKCβII or PKCθ, were decreased in the cytosolic fractions of XLKO samples compared to those in cytosolic fractions of samples from wild-type mice (Fig. 5B and fig. S4, A and B). PKCδ abundance was also markedly decreased in the membrane fractions of XLKO samples, whereas the abundances of PKCα and PKCζ were only slightly reduced (Fig. 5, B to E). Moreover, the abundances of PKCδ, PKCα, and PKCζ after PTH treatment were substantially decreased in both the cytosolic and membrane fractions of XLKO samples compared to those of wild-type samples (Fig. 5, B to E). Western blotting analysis indicated no reduction in the abundance of phosphorylated extracellular signal–regulated kinase 1 (ERK1) and ERK2 in the proximal tubules from XLKO mice either under basal conditions or after stimulation with PTH (fig. S4, C and D), whereas the amounts of phosphorylated PKA targets were slightly increased in membrane fractions after stimulation with PTH (Fig. 5B and fig. S4E).

Hyperphosphatemia and reduced $G_{q/11}$ signaling in XLKO mice are rescued by overexpression of XLαs specifically in proximal tubules

Knockout of the gene encoding XLαs in XLKO mice ablates not only XLαs, but also its variants in all tissues (9). To determine whether the proximal tubule–specific overexpression of XLαs could rescue the hyperphosphatemia phenotype of P2 XLKO mice, we crossed XLKO mice to transgenic mice in which XLαs expression was targeted to the renal proximal tubule with the promoter of the gene encoding the type I rat γ-glutamyltranspeptidase promoter (rptXLαs mice) (25). We found that this promoter was active at the P2 stage and that the abundance of *XLαs* mRNA in rptXLαs mice was 12-fold higher than that in wild-type littermates (Fig. 6A). Whereas the XLKO offspring from these matings showed hyperphosphatemia, rptXLαs offspring tended to have reduced

concentrations of serum phosphate (Fig. 6B). Serum phosphate concentrations were statistically significantly lower in the XLKO:rptXLαs offspring than in the XLKO offspring, and these concentrations were comparable to those in wild-type littermates (Fig. 6B). In addition, the increase in *Cyp27b1* expression observed in XLKO mice was effectively reversed by transgenic overexpression of XLαs (Fig. 6C), although the expression of *Cyp24a1* was still increased in the XLKO:rptXLαs mice (Fig. 6D). The reduced abundance of *Kid1* mRNA in XLKO mice was also fully rescued by overexpression of XLαs in proximal tubules (Fig. 6E). Western blotting analysis revealed that the reduction in the abundances of PKCδ, PKCα, and PKCζ in the proximal tubules of XLKO mice was also rescued by the proximal tubule–specific overexpression of XLαs (Fig. 6, F to I). In particular, overexpression of XLαs in the proximal tubule substantially increased the membrane abundance of PKCδ, which was evident in both rptXLαs and XLKO:rptXLαs pups (Fig. 6, F and G).

XLαs expression enhances the basal and agonist-stimulated amounts of IP_1

Basal and PTH-stimulated concentrations of IP_1 were statistically significantly increased in proximal tubule–enriched cortices isolated from P2 rptXLαs mice compared to those in similar cortices isolated from wild-type littermates (Fig. 7A). Concordant with these results, transient transfection of human embryonic kidney (HEK) 293 cells stably expressing the PTH receptor with increasing amounts of plasmid encoding XLαs resulted in a dose-dependent increase in basal IP_1 concentrations (Fig. 7B). Moreover, cells transfected with either control plasmid or plasmid encoding XLαs responded to PTH, but the overexpression of XLαs substantially enhanced the generation of IP_1 in response to different concentrations of PTH (Fig. 7C). Furthermore, overexpression of XLαs in these cells also enhanced the amount of IP_1 generated in response to thrombin, another agonist that acts through its own endogenous G_q-coupled receptor (Fig. 7D). In addition, we examined a guanosine triphosphatase (GTPase) deficient mutant of XLαs (XLαs-R543H), which shows constitutive activity with respect to cAMP generation (24). As expected, HEK 293 cells transiently expressing this mutant XLαs displayed increased basal cAMP generation compared to those cells expressing wild-type XLαs (Fig. 7E). Similarly, basal IP_1 concentrations were substantially greater in HEK 293 cells expressing XLαs-R543H than in those expressing wild-type XLαs (Fig. 7F).

To determine whether XLαs could mimic the actions of $G_{q/11}$ proteins, we expressed XLαs in HEK 293 cells in which G_q and G_{11} were both ablated through the use of the CRISPR (clustered regularly interspaced short palindromic repeats)/Cas9 system(CRISPR-associated). Thrombin stimulated a 2.55-fold increase in IP_1 generation in native HEK 293 cells compared to that in unstimulated cells (Fig. 7G), whereas it failed to stimulate IP_1 generation in $G_{q/11}$-deficient HEK 293 cells that were transfected with control plasmid (Fig. 7H). Transient transfection of the $G_{q/11}$-deficient HEK 293 cells with plasmid encoding either Gαq or Gα11 led to an increase in basal IP_1 concentrations and rescued the thrombin-stimulated generation of IP_1 (Fig 7H). In $G_{q/11}$-deficient HEK 293 cells transfected with plasmid encoding XLαs, the basal IP_1 concentration was 3.39-fold greater than that in cells transfected with the control plasmid, and thrombin stimulated a 1.81-fold increase in IP_1

abundance compared to that in unstimulated $G_{q/11}$-deficient cells expressing XLαs (Fig. 7H).

DISCUSSION

We investigated the role of XLαs, a variant of Gαs, by focusing on the action of PTH, and our data suggest that XLαs is essential for the PTH-mediated regulation of phosphate-handling in the renal proximal tubule during early postnatal development. Whereas this role of XLαs appears to be similar to that of Gαs in the same context, we found that the ablation of XLαs in mice repressed $G_{q/11}$-mediated signaling rather than G_s-mediated signaling. Our additional results suggest that XLαs promotes basal and agonist-stimulated signaling by $G_{q/11}$ proteins.

By stimulating at least two signaling pathways, which are mediated by G_s and $G_{q/11}$ proteins, PTH inhibits renal phosphate reabsorption by decreasing the abundance of Npt2a protein. The hyperphosphatemia in XLKO mice is thus consistent with an increase in the amount of Npt2a at steady-state and the blunted PTH-induced reduction in Npt2a abundance. FGF23 also decreases the abundance of Npt2a (32), and therefore, the increased Npt2a abundance would be consistent with the reduction in the amount of FGF23 in XLKO mice. However, a role for reduced FGF23 in P2 XLKO mice is unlikely because complete ablation of FGF23 in mice does not lead to alterations in serum phosphate and calcium concentrations until after P6 (33, 34). PTH also increases the synthesis of $1,25(OH)_2D$ by inducing the expression of *Cyp27b1*, but this effect depends largely on Gs-dependent signaling (27, 35). Because the serum PTH concentration was increased in XLKO pups compared to that in wild-type pups, and because this was concurrent with markedly increased amounts of renal *Cyp27b1* mRNA and $1,25(OH)_2D$, it is possible that the action of PTH on *Cyp27b1* expression is somewhat preserved in the absence of XLαs. In support of this possibility was the tendency of renal *Cyp27b1* mRNA abundance to increase even more than the already enhanced amounts in response to PTH in XLKO pups (Fig. 4A). A reduction in the amount serum FGF23 is unlikely to account for the increased amount of $1,25(OH)_2D$ in P2 XLKO pups, because FGF23-deficient mice do not display increased amounts of $1,25(OH)_2D$ until after P10 (33). $1,25(OH)_2D$ stimulates the expression of *Cyp24a1*, which would thus explain the increased renal abundance of *Cyp24a1* mRNA in XLKO pups.

The hypocalcemia in XLKO pups is more difficult to explain, given their increased amounts of $1,25(OH)_2D$, which normally enhances Ca^{2+} absorption in the gut. In newborns, however, deficiency in $1,25(OH)_2D$ or the loss of its receptor does not lead to hypocalcemia, which suggests that this hormone is not essential for regulating serum Ca^{2+} concentrations during early postnatal life (36). It is possible that the reduced serum concentration of Ca^{2+} in XLKO pups is secondary to hyperphosphatemia or reflects the poor feeding of the XLKO pups (9). In addition, PTH enhances the reabsorption of Ca^{2+} in the renal distal tubule (22). Because we detected XLαs protein in this part of the nephron, PTH-induced reabsorption of Ca^{2+} may be impaired in P2 XLKO mice, thus contributing to the hypocalcemia despite the presence of increased amounts of PTH in the serum of these mice.

The PTH resistance in XLKO pups was observed in the presence of intact, and modestly increased, Gαs abundance and an enhanced PTH-stimulated cAMP response. In contrast, basal and PTH-stimulated IP_3 signaling and the abundances of certain PKC isoforms were repressed. In addition, overexpression of XLαs in the proximal tubules of XLKO pups rescued both the hyperphosphatemia and the diminished generation of IP_1. It thus appears that the impaired responsiveness of Npt2a to PTH in the proximal tubules of XLKO mice, and the resultant changes in serum biochemistries of XLKO pups, are at least partly a result of the impaired activation of IP_3-DAG signaling. Together with the results of our cell culture experiments, these findings suggest that XLαs serves as a $G\alpha_{q/11}$-like signaling protein and that it mediates the PTH-induced inhibition of phosphate reabsorption from the glomerular filtrate. Previous studies showed that the $G_{q/11}$ signaling pathway and the activation of PKC play crucial roles in the PTH-stimulated internalization of Npt2a and regulation of phosphate homeostasis (37-39). Our findings confirm the importance of this signaling pathway to the renal actions of PTH, and they identify XLαs as an indispensable mediator of those actions during early postnatal development. Given that XLKO mice that survive to weaning show normal concentrations of phosphate, Ca^{2+}, and PTH in the serum (14), the phenotypes of XLKO pups are similar to the clinical findings of patients with transient neonatal pseudohypoparathyroidism, who show hypocalcemia, hyperphosphatemia, and increased serum PTH concentrations during early postnatal life (40, 41). Whether these patients have mutations in exon 1 of their paternal *GNAS* XLαs or in genes encoding the signaling partners of XLαs should be investigated.

Despite having increased serum PTH concentrations and Gαs protein abundance in renal brush border membranes, XLKO mice had baseline urinary cAMP concentrations that were indistinguishable from those of wild-type mice. This finding may reflect a lack of sensitivity of our cAMP measurement assay. Alternatively, XLKO pups may have developed adaptive changes to prevent increases in urinary cAMP concentration at steady-state, such as desensitization of the mechanism responsible for the efflux of cAMP into the urine. The quantities of phosphorylated PKA substrates in the proximal tubules of unstimulated XLKO and wild-type mice were similar, suggesting that other adaptive changes may have occurred, such as in the relative amounts of cAMP phosphodiesterases (Fig. 5 and fig. S4E). In contrast, phosphorylated PKA substrates were substantially more abundant in the proximal tubule membranes of PTH-stimulated XLKO mice than in those of PTH-stimulated wild-type mice. It is possible that the exchange protein activated by cAMP (Epac) is also activated more robustly in the proximal tubules of XLKO mice than in the proximal tubules of wild-type mice, particularly after receptor stimulation. Epac plays important roles in proximal tubules through its stimulation of ERK1/2 signaling (42, 43); however, the abundance of phosphorylated ERK1/2 was not altered in the proximal tubules of XLKO mice (fig. S4, C and D). Moreover, a study suggests that Epac activation is not involved in renal phosphate-handling or the regulation of Npt2a (44), arguing against the possibility that enhanced Epac activity contributes to the hyperphosphatemia observed in XLKO pups.

Consistent with the marked identity between the amino acid sequences of XLαs and Gαs, in vitro overexpression experiments indicate that XLαs stimulates both basal and receptor-activated generation of cAMP (24, 25); however, no cAMP-independent cellular functions

have hitherto been assigned to XLαs. Our study suggests that even though it is a Gαs-like protein, XLαs promotes the $G_{q/11}$ signaling pathway in vivo. Thus, the *GNAS* complex locus presents an interesting paradigm in which a single gene encoding a G protein α-subunit encodes partially identical products that stimulate two different G protein– mediated pathways. Unlike in the regulation of PTH-mediated phosphate-handling, the Gs- and $G_{q/11}$-dependent signaling pathways mediate opposing responses in many tissues, such as platelets and airway smooth muscles (45, 46). Consistent with these actions, previous studies have indicated that Gαs and XLαs have opposing roles in vivo (17, 47).

The effect of XLαs on $G_{q/11}$ signaling and PKC isoform abundance could be developmental, but our experiments with transiently transfected cells suggest that XLαs directly enhances the activation of PLC-β. Moreover, results from experiments with the GTPase-deficient XLαs mutant, which is analogous to the Gαs mutant R201H that is found in multiple benign and malignant tumors (3), indicate that this action of XLαs is also limited by its intrinsic GTPase activity. In addition, our findings obtained from experiments with $G_{q/11}$-deficient cells suggest that XLαs stimulates IP_3 generation at least partly by mimicking the actions of $G\alpha_q$ and $G\alpha_{11}$. It could be argued that XLαs promotes the $G_{q/11}$ signaling pathway by increasing the abundance of cAMP, because cAMP signaling in some cells can stimulate certain PLC isozymes (48). In overexpression experiments, a similar mechanism could perhaps be involved in the XLαs-mediated generation of IP_3, particularly under basal conditions; however, thrombin receptors do not couple to G_s proteins (49), and therefore thrombin-induced IP_3 generation in XLαs-expressing, $G_{q/11}$-deficient cells is unlikely to be secondary to cAMP generation. Our findings from in vivo experiments also argue against the involvement of a cAMP-dependent mechanism, because XLKO pups showed increased PTH-stimulated generation of cAMP in the proximal tubule despite having diminished $G_{q/11}$-mediated signaling.

PKCs are divided into three subfamilies: conventional, novel, and atypical. Conventional PKCs, such as PKCα, and novel PKCs, such as PKCδ, require DAG for their activation, and are thus downstream of $G_{q/11}$ signaling (50). The inhibited generation of IP_3, as well as the decreased abundances of PKCδ and PKCα, in the proximal tubules of P2 XLKO mice suggest that XLαs plays a stimulatory role in $G_{q/11}$ signaling. On the other hand, PKCζ, which is an atypical PKC that does not require DAG or Ca^{2+} for activation (51), was also reduced in abundance in samples from XLKO mice, suggesting that XLαs might also regulate the abundance of atypical PKCs through an as-yet-undefined mechanism. PTH stimulates PKC activation in a PLC-independent manner (52), which might possibly be mediated by XLαs.

That loss of XLαs increased the PTH-stimulated generation of cAMP is consistent with data from experiments with brown adipose tissue (BAT) from XLKO mice, in which basal and isoproterenol-stimulated cAMP generation were enhanced compared to those in BAT from wild-type mice (9). Our results suggest that the increased production of cAMP in the proximal tubules of XLKO mice is at least partly a result of increased Gαs abundance. It is tempting to speculate that the changes in Gαs abundance reflect a physiological response to help counteract the hyperphosphatemia. The change in Gαs abundance in proximal tubules from XLKO mice may also result from the loss of a potential regulatory mechanism

involving an interaction in cis between the paternal *XLαs* transcript and the downstream Gαs promoter, because a similar mechanism involving another paternally expressed upstream *GNAS* transcript (A/B) and the Gαs promoter has been proposed (53).

GNAS is a highly complex locus, and XLαs itself has multiple variants and alternative translational products (6, 18-21). The XLKO mice have a deletion in extra-large exon 1, thus ablating all of these variants (9). Thus, the PTH-resistant phenotype of XLKO pups could reflect n a deficiency in one or more of these proteins. However, the phenotype was rescued by overexpressing XLαs in the proximal tubule, and it is therefore likely that the phenotype reflects a specific deficiency in XLαs, rather than its other variants, in this tissue. Note that the XLKO:rptXLαs pups appeared grossly indistinguishable from their XLKO littermates and showed a similar degree of early postnatal lethality, indicating that other XLαs variants could be responsible for these other defects.

In summary, our study revealed a hitherto unknown function of the large Gαs variant XLαs, demonstrating that this imprinted protein can enhance the $G_{q/11}$ signaling pathway. Our studies with XLαs-deficient mice also suggest that XLαs is required for the action of PTH in the proximal tubules of early postnatal mice with respect to phosphate-handling. These findings have broad implications regarding the pathogenesis of human diseases caused by *GNAS* mutations or copy number variations.

MATERIALS AND METHODS

Mice

XLKO mice and rptXLαs mice (9, 25) were maintained in a CD1 genetic background. All the animal experiments were conducted in accordance with the accepted standards of the Institutional Animal Care and Use Committee, and the studies were approved by the Massachusetts General Hospital Subcommittee on Research Animal Care.

Expression plasmids

Construction of plasmids encoding XLαs and the GTPase-deficient XLαs mutant XLαs-R543H was described previously (20, 24). Plasmids encoding Gαq and Gα11 plasmids were obtained from cDNA.org.

cDNA synthesis and qRT-PCR analysis

Total RNA isolated from the kidneys of P2 WT, XLKO, rptXLαs, and XLKO:rptXLαs mice was prepared with the RNeasy Plus Mini Kit (Qiagen), and cDNA was synthesized with the ProtoScript II First stand cDNA synthesis kit (New England Biolabs) as previously described (54). qRT-PCR analysis was performed with specific primers (table S1) and FastStart Universal SYBR Green Master (Roche) with *Actb* (*β-actin)* as a reference gene.

Immunofluorescence microscopy

Kidneys were isolated from P2 XLKO and WT littermates, fixed, and serially sectioned at 5 μm. Sections were incubated with polyclonal antiserum against mouse XLαs (25) at a 1:500 dilution, antibody specific for the N-terminal region of Gαs encoded by exon 1 (1:500) (a

gift of S. Mollner, Germany) (4), or antibody against Calbindin D-28K (Sigma) at 4°C overnight. Sections were then incubated with Alexa Fluor 568–conjugated donkey anti-rabbit antibody and Alexa Fluor 488–conjugated phalloidin, or with Alexa Fluor 488–conjugated goat anti-mouse antibody (Life technologies) at room temperature for one hour (24). Immunoreactivity was visualized and analyzed with a Zeiss LSM 510 Confocal Microscope and Zeiss Zen software.

Measurement of serum biochemistries

Blood samples for the analysis of serum concentrations of phosphate, Ca^{2+}, PTH, and $1,25(OH)_2D$ were obtained from the carotid artery and were processed as described previously (25). Serum FGF23 concentrations were measured with the Mouse/Rat FGF-23 (C-Term) ELISA kit (Immutopics). To determine the effect of PTH on cAMP generation in vivo, urine was collected 15 min after mice were injected s.c. with vehicle or PTH(1-34) (50 nmol/kg), and the concentration of cAMP was quantified as described previously (14). The PTH-induced reduction in the concentration of serum phosphate was measured two hours after mice were injected with PTH(1-34) or vehicle as previously described (25).

Isolation and Western blotting analysis of renal brush border membranes

Brush border membrane portions were isolated from the kidneys of P2 mice as described previously (55) with minor modifications. Isolated brush border membrane proteins were lysed in a Tris-buffered solution containing 150 mM NaCl and 1% Triton and a protease inhibitor cocktail (Roche). Measurement of protein concentrations in the samples and Western blotting analysis with antibodies specific for Npt2a, Npt2c (56), and Gαs (Millipore) were performed as described previously (25).

Isolation of proximal tubule–enriched cortices and IP_1 assays

Proximal tubule–enriched renal cortices were prepared by collagenase digestion of P2 mouse kidneys and isolation on a Percoll gradient as described previously (57). Proximal tubules from P2 WT, XLKO, or rptXLαs mice were treated with different concentrations of PTH(1-34) for 30 minutes in the presence of $LiCl_2$ and then were analyzed to determine the amount of IP_1, a downstream metabolite of IP_3, with the IP_1 HTRF assay kit (Cisbio). HEK 293 cells stably expressing the PTHR (a gift of T. Gardella, MGH) were transfected with plasmids encoding XLαs or XLαs-R543H and incubated for 30 min in the presence or absence of PTH(1-34) before IP_1 concentrations were measured. Parental WT and $G\alpha_{q/11}{}^{-/-}$ HEK 293 cells (a gift of A. Inoue, Tohoku University) were transfected with pcDNA or plasmids encoding XLαs, Gαq, or Gα11 and then incubated for 30 min in the presence or absence of thrombin before IP_1 concentrations were measured.

cAMP signaling assays

Signaling through the cAMP and PKA pathway was assessed in experiments with HEK 293 cells stably transfected with the Glosensor cAMP reporter plasmid and with plasmid encoding PTHR and then transiently transfected with plasmids encoding XLαs or XLαs-R543H. For assays, confluent cells in 96-well plates were treated with luciferin and 2 mM

IBMX (3-isobutyl-1-methylxanthine) for 30 min before luminescence was measured as previously described (58).

Cell fractionation and analysis of PKC isoforms

Proximal tubule–enriched renal cortices were subjected to cell fractionation by ultracentrifuge to separate cytosolic and membrane fractions (59). Protein lysates were resolved by 10% SDS-polyacrylamide gel electrophoresis (SDS-PAGE) and transferred to nitrocellulose membranes (Bio-rad). Western blots were then incubated with antibodies directed against specific PKC isoforms, phosphorylated substrates of PKA, and phosphorylated ERK1/2 (Cell signaling). Antibodies against actin (Santa Cruz) and the Na-K ATPase (Cell signaling) were used to identify cytosolic and membrane fractions. Densitometric analysis of Western blots was performed with ImageJ software.

Statistical analysis

The means ± SEM of multiple independent measurements were calculated. To determine statistical significance, Leven's F-test was first performed to assess equality of variances. If variances were equal, the Student's t-test (two-tailed) assuming equal variance was used for comparing two means, whereas one-way ANOVA followed by Tukey's multiple comparison test was used for comparing three or more groups. Welch's t-test (two-tailed) was used for comparisons between two means with unequal variances. The same test was used for multiple comparisons involving groups with unequal variances, followed by Bonferroni correction (that is, *P* values were multiplied by the number of comparisons). Statistical significance is represented as follows: $*P < 0.05$, $**P < 0.01$, $***P < 0.001$.

Supplementary Material

Refer to Web version on PubMed Central for supplementary material.

Acknowledgments

We thank T. Gardella and H. Jüppner (MGH) for insightful discussions and H. M. Kronenberg (MGH) for critically reviewing the manuscript. The abundance of IP_1 was measured at the Massachusetts General Hospital Endocrine Unit Center for Skeletal Research, Bone Cell and Signaling Core. Human PTH (1–34) was synthesized by the Peptide/Protein Core Facility at Massachusetts General Hospital. **Funding:** This work was conducted with support from Harvard Catalyst: The Harvard Clinical and Translational Science Center (National Center for Research Resources and the National Center for Advancing Translational Sciences, National Institutes of Health Award UL1 TR001102) and financial contributions from Harvard University and its affiliated academic healthcare centers. The studies were funded in part by a research grant from NIH/NIDDK (RO1DK073911 to M.B.). The Massachusetts General Hospital Endocrine Unit Center for Skeletal Research was funded by a grant from NIH/NIAMS (P30 AR066261).

REFERENCES and NOTES

1. Turan S, Bastepe M. The GNAS complex locus and human diseases associated with loss-of-function mutations or epimutations within this imprinted gene. Horm Res Paediatr. 2013; 80:229–41. [PubMed: 24107509]
2. Plagge A, Kelsey G, Germain-Lee EL. Physiological functions of the imprinted Gnas locus and its protein variants Galpha(s) and XLalpha(s) in human and mouse. J Endocrinol. 2008; 196:193–214. [PubMed: 18252944]

3. Weinstein LS, Yu S, Warner DR, Liu J. Endocrine manifestations of stimulatory G protein alpha-subunit mutations and the role of genomic imprinting. Endocr Rev. 2001; 22:675–705. [PubMed: 11588148]

4. Kehlenbach RH, Matthey J, Huttner WB. XL alpha s is a new type of G protein. Nature. 1994; 372:804–9. [PubMed: 7997272]

5. Yu S, Yu D, Lee E, Eckhaus M, Lee R, Corria Z, Accili D, Westphal H, Weinstein LS. Variable and tissue-specific hormone resistance in heterotrimeric Gs protein alpha-subunit (Gsalpha) knockout mice is due to tissue-specific imprinting of the gsalpha gene. Proc Natl Acad Sci U S A. 1998; 95:8715–20. [PubMed: 9671744]

6. Hayward BE, Kamiya M, Strain L, Moran V, Campbell R, Hayashizaki Y, Bonthron DT. The human GNAS1 gene is imprinted and encodes distinct paternally and biallelically expressed G proteins. Proc Natl Acad Sci U S A. 1998; 95:10038–43. [PubMed: 9707596]

7. Peters J, Wroe SF, Wells CA, Miller HJ, Bodle D, Beechey CV, Williamson CM, Kelsey G. A cluster of oppositely imprinted transcripts at the Gnas locus in the distal imprinting region of mouse chromosome 2. Proc Natl Acad Sci U S A. 1999; 96:3830–5. [PubMed: 10097123]

8. Richard N, Molin A, Coudray N, Rault-Guillaume P, Juppner H, Kottler ML. Paternal GNAS mutations lead to severe intrauterine growth retardation (IUGR) and provide evidence for a role of XLalphas in fetal development. J Clin Endocrinol Metab. 2013; 98:E1549–56. [PubMed: 23884777]

9. Plagge A, Gordon E, Dean W, Boiani R, Cinti S, Peters J, Kelsey G. The imprinted signaling protein XL alpha s is required for postnatal adaptation to feeding. Nat Genet. 2004; 36:818–26. [PubMed: 15273686]

10. Genevieve D, Sanlaville D, Faivre L, Kottler ML, Jambou M, Gosset P, Boustani-Samara D, Pinto G, Ozilou C, Abeguile G, Munnich A, Romana S, Raoul O, Cormier-Daire V, Vekemans M. Paternal deletion of the GNAS imprinted locus (including Gnasxl) in two girls presenting with severe pre- and post-natal growth retardation and intractable feeding difficulties. Eur J Hum Genet. 2005; 13:1033–9. [PubMed: 15915160]

11. Aldred MA, Aftimos S, Hall C, Waters KS, Thakker RV, Trembath RC, Brueton L. Constitutional deletion of chromosome 20q in two patients affected with albright hereditary osteodystrophy. Am J Med Genet. 2002; 113:167–72. [PubMed: 12407707]

12. Izzi B, Francois I, Labarque V, Thys C, Wittevrongel C, Devriendt K, Legius E, Van den Bruel A, D'Hooghe M, Lambrechts D, de Zegher F, Van Geet C, Freson K. Methylation defect in imprinted genes detected in patients with an Albright's hereditary osteodystrophy like phenotype and platelet Gs hypofunction. PLoS One. 2012; 7:e38579. [PubMed: 22679513]

13. Garcia-Murillas I, Sharpe R, Pearson A, Campbell J, Natrajan R, Ashworth A, Turner NC. An siRNA screen identifies the GNAS locus as a driver in 20q amplified breast cancer. Oncogene. 2014; 33:2478–86. [PubMed: 23752180]

14. Fernandez-Rebollo E, Maeda A, Reyes M, Turan S, Frohlich LF, Plagge A, Kelsey G, Juppner H, Bastepe M. Loss of XLalphas (extra-large alphas) imprinting results in early postnatal hypoglycemia and lethality in a mouse model of pseudohypoparathyroidism Ib. Proc Natl Acad Sci U S A. 2012; 109:6638–43. [PubMed: 22496590]

15. Klemke M, Pasolli HA, Kehlenbach RH, Offermanns S, Schultz G, Huttner WB. Characterization of the extra-large G protein alpha-subunit XLalphas. II. Signal transduction properties. J Biol Chem. 2000; 275:33633–40. [PubMed: 10931851]

16. Bastepe M, Gunes Y, Perez-Villamil B, Hunzelman J, Weinstein LS, Juppner H. Receptor-mediated adenylyl cyclase activation through XLalpha(s), the extra-large variant of the stimulatory G protein alpha-subunit. Mol Endocrinol. 2002; 16:1912–9. [PubMed: 12145344]

17. Xie T, Plagge A, Gavrilova O, Pack S, Jou W, Lai EW, Frontera M, Kelsey G, Weinstein LS. The alternative stimulatory G protein alpha-subunit XLalphas is a critical regulator of energy and glucose metabolism and sympathetic nerve activity in adult mice. J Biol Chem. 2006; 281:18989–99. [PubMed: 16672216]

18. Pasolli HA, Klemke M, Kehlenbach RH, Wang Y, Huttner WB. Characterization of the extra-large G protein alpha-subunit XLalphas. I. Tissue distribution and subcellular localization. J Biol Chem. 2000; 275:33622–32. [PubMed: 10931823]

19. Klemke M, Kehlenbach RH, Huttner WB. Two overlapping reading frames in a single exon encode interacting proteins--a novel way of gene usage. EMBO J. 2001; 20:3849–60. [PubMed: 11447126]

20. Aydin C, Aytan N, Mahon MJ, Tawfeek HA, Kowall NW, Dedeoglu A, Bastepe M. Extralarge XL(alpha)s (XXL(alpha)s), a variant of stimulatory G protein alpha-subunit (Gs(alpha)), is a distinct, membrane-anchored GNAS product that can mimic Gs(alpha). Endocrinology. 2009; 150:3567–75. [PubMed: 19423757]

21. Abramowitz J, Grenet D, Birnbaumer M, Torres HN, Birnbaumer L. XLalphas, the extra-long form of the alpha-subunit of the Gs G protein, is significantly longer than suspected, and so is its companion Alex. Proc Natl Acad Sci U S A. 2004; 101:8366–71. [PubMed: 15148396]

22. Kronenberg, H.; Williams, RH. Williams textbook of endocrinology. Saunders/Elsevier; Philadelphia: 2008. p. xixp. 1911

23. Bringhurst FR, Juppner H, Guo J, Urena P, Potts JT Jr. Kronenberg HM, Abou-Samra AB, Segre GV. Cloned, stably expressed parathyroid hormone (PTH)/PTH-related peptide receptors activate multiple messenger signals and biological responses in LLC-PK1 kidney cells. Endocrinology. 1993; 132:2090–8. [PubMed: 8386606]

24. Liu Z, Turan S, Wehbi VL, Vilardaga JP, Bastepe M. Extra-long Galphas variant XLalphas protein escapes activation-induced subcellular redistribution and is able to provide sustained signaling. J Biol Chem. 2011; 286:38558–69. [PubMed: 21890629]

25. Liu Z, Segawa H, Aydin C, Reyes M, Erben RG, Weinstein LS, Chen M, Marshansky V, Frohlich LF, Bastepe M. Transgenic overexpression of the extra-large Gsalpha variant XLalphas enhances Gsalpha-mediated responses in the mouse renal proximal tubule in vivo. Endocrinology. 2011; 152:1222–33. [PubMed: 21303955]

26. Shimada T, Hasegawa H, Yamazaki Y, Muto T, Hino R, Takeuchi Y, Fujita T, Nakahara K, Fukumoto S, Yamashita T. FGF-23 is a potent regulator of vitamin D metabolism and phosphate homeostasis. J Bone Miner Res. 2004; 19:429–35. [PubMed: 15040831]

27. Brenza HL, Kimmel-Jehan C, Jehan F, Shinki T, Wakino S, Anazawa H, Suda T, DeLuca HF. Parathyroid hormone activation of the 25-hydroxyvitamin D3-1alpha-hydroxylase gene promoter. Proc Natl Acad Sci U S A. 1998; 95:1387–91. [PubMed: 9465024]

28. Murer H, Lotscher M, Kaissling B, Levi M, Kempson SA, Biber J. Renal brush border membrane Na/Pi-cotransport: molecular aspects in PTH-dependent and dietary regulation. Kidney Int. 1996; 49:1769–73. [PubMed: 8743494]

29. Chase LR, Melson GL, Aurbach GD. Pseudohypoparathyroidism: defective excretion of 3′,5′-AMP in response to parathyroid hormone. J Clin Invest. 1969; 48:1832–44. [PubMed: 4309802]

30. Dunlay R, Hruska K. PTH receptor coupling to phospholipase C is an alternate pathway of signal transduction in bone and kidney. Am J Physiol. 1990; 258:F223–31. [PubMed: 2155534]

31. Guo J, Song L, Liu M, Segawa H, Miyamoto K, Bringhurst FR, Kronenberg HM, Juppner H. Activation of a non-cAMP/PKA signaling pathway downstream of the PTH/PTHrP receptor is essential for a sustained hypophosphatemic response to PTH infusion in male mice. Endocrinology. 2013; 154:1680–9. [PubMed: 23515284]

32. Gattineni J, Bates C, Twombley K, Dwarakanath V, Robinson ML, Goetz R, Mohammadi M, Baum M. FGF23 decreases renal NaPi-2a and NaPi-2c expression and induces hypophosphatemia in vivo predominantly via FGF receptor 1. Am J Physiol Renal Physiol. 2009; 297:F282–91. [PubMed: 19515808]

33. Shimada T, Kakitani M, Yamazaki Y, Hasegawa H, Takeuchi Y, Fujita T, Fukumoto S, Tomizuka K, Yamashita T. Targeted ablation of Fgf23 demonstrates an essential physiological role of FGF23 in phosphate and vitamin D metabolism. J Clin Invest. 2004; 113:561–8. [PubMed: 14966565]

34. Ma Y, Samaraweera M, Cooke-Hubley S, Kirby BJ, Karaplis AC, Lanske B, Kovacs CS. Neither absence nor excess of FGF23 disturbs murine fetal-placental phosphorus homeostasis or prenatal skeletal development and mineralization. Endocrinology. 2014; 155:1596–605. [PubMed: 24601885]

35. Murayama A, Takeyama K, Kitanaka S, Kodera Y, Kawaguchi Y, Hosoya T, Kato S. Positive and negative regulations of the renal 25-hydroxyvitamin D3 1alpha-hydroxylase gene by parathyroid

hormone, calcitonin, and 1alpha,25(OH)2D3 in intact animals. Endocrinology. 1999; 140:2224–31. [PubMed: 10218975]

36. Kovacs CS. The role of vitamin D in pregnancy and lactation: insights from animal models and clinical studies. Annu Rev Nutr. 2012; 32:97–123. [PubMed: 22483092]
37. Capuano P, Bacic D, Roos M, Gisler SM, Stange G, Biber J, Kaissling B, Weinman EJ, Shenolikar S, Wagner CA, Murer H. Defective coupling of apical PTH receptors to phospholipase C prevents internalization of the Na+-phosphate cotransporter NaPi-IIa in Nherf1-deficient mice. Am J Physiol Cell Physiol. 2007; 292:C927–34. [PubMed: 16987995]
38. Traebert M, Volkl H, Biber J, Murer H, Kaissling B. Luminal and contraluminal action of 1-34 and 3-34 PTH peptides on renal type IIa Na-P(i) cotransporter. Am J Physiol Renal Physiol. 2000; 278:F792–8. [PubMed: 10807591]
39. Forster IC, Hernando N, Biber J, Murer H. Proximal tubular handling of phosphate: A molecular perspective. Kidney Int. 2006; 70:1548–59. [PubMed: 16955105]
40. Minagawa M, Yasuda T, Kobayashi Y, Niimi H. Transient pseudohypoparathyroidism of the neonate. Eur J Endocrinol. 1995; 133:151–5. [PubMed: 7655638]
41. Manzar S. Transient pseudohypoparathyroidism and neonatal seizure. J Trop Pediatr. 2001; 47:113–4. [PubMed: 11336128]
42. Carraro-Lacroix LR, Malnic G, Girardi AC. Regulation of Na+/H+ exchanger NHE3 by glucagon-like peptide 1 receptor agonist exendin-4 in renal proximal tubule cells. Am J Physiol Renal Physiol. 2009; 297:F1647–55. [PubMed: 19776173]
43. Lee YJ, Kim MO, Ryu JM, Han HJ. Regulation of SGLT expression and localization through Epac/PKA-dependent caveolin-1 and F-actin activation in renal proximal tubule cells. Biochim Biophys Acta. 2012; 1823:971–82. [PubMed: 22230192]
44. Honegger KJ, Capuano P, Winter C, Bacic D, Stange G, Wagner CA, Biber J, Murer H, Hernando N. Regulation of sodium-proton exchanger isoform 3 (NHE3) by PKA and exchange protein directly activated by cAMP (EPAC). Proc Natl Acad Sci U S A. 2006; 103:803–8. [PubMed: 16407144]
45. Brass LF, Hoxie JA, Kieber-Emmons T, Manning DR, Poncz M, Woolkalis M. Agonist receptors and G proteins as mediators of platelet activation. Adv Exp Med Biol. 1993; 344:17–36. [PubMed: 8209785]
46. Billington CK, Penn RB. Signaling and regulation of G protein-coupled receptors in airway smooth muscle. Respir Res. 2003; 4:2. [PubMed: 12648290]
47. Chen M, Gavrilova O, Liu J, Xie T, Deng C, Nguyen AT, Nackers LM, Lorenzo J, Shen L, Weinstein LS. Alternative Gnas gene products have opposite effects on glucose and lipid metabolism. Proc Natl Acad Sci U S A. 2005; 102:7386–91. [PubMed: 15883378]
48. Hui X, Reither G, Kaestner L, Lipp P. Targeted activation of conventional and novel protein kinases C through differential translocation patterns. Mol Cell Biol. 2014; 34:2370–81. [PubMed: 24732802]
49. Verrall S, Ishii M, Chen M, Wang L, Tram T, Coughlin SR. The thrombin receptor second cytoplasmic loop confers coupling to Gq-like G proteins in chimeric receptors. Additional evidence for a common transmembrane signaling and G protein coupling mechanism in G protein-coupled receptors. J Biol Chem. 1997; 272:6898–902. [PubMed: 9054376]
50. Gschwendt M. Protein kinase C delta. Eur J Biochem. 1999; 259:555–64. [PubMed: 10092837]
51. Hirai T, Chida K. Protein kinase Czeta (PKCzeta): activation mechanisms and cellular functions. J Biochem. 2003; 133:1–7. [PubMed: 12761192]
52. Takasu H, Guo J, Bringhurst FR. Dual signaling and ligand selectivity of the human PTH/PTHrP receptor. J Bone Miner Res. 1999; 14:11–20. [PubMed: 9893061]
53. Eaton SA, Williamson CM, Ball ST, Beechey CV, Moir L, Edwards J, Teboul L, Maconochie M, Peters J. New mutations at the imprinted Gnas cluster show gene dosage effects of Gsalpha in postnatal growth and implicate XLalphas in bone and fat metabolism but not in suckling. Mol Cell Biol. 2012; 32:1017–29. [PubMed: 22215617]
54. He Q, Yang X, Gong Y, Kovalenko D, Canalis E, Rosen CJ, Friesel RE. Deficiency of Sef is associated with increased postnatal cortical bone mass by regulating Runx2 activity. J Bone Miner Res. 2014; 29:1217–31. [PubMed: 24127237]

55. Biber J, Stieger B, Stange G, Murer H. Isolation of renal proximal tubular brush-border membranes. Nat Protoc. 2007; 2:1356–9. [PubMed: 17545973]

56. Masuda M, Yamamoto H, Kozai M, Tanaka S, Ishiguro M, Takei Y, Nakahashi O, Ikeda S, Uebanso T, Taketani Y, Segawa H, Miyamoto K, Takeda E. Regulation of renal sodium-dependent phosphate co-transporter genes (Npt2a and Npt2c) by all-trans-retinoic acid and its receptors. Biochem J. 2010; 429:583–92. [PubMed: 20507281]

57. Doctor RB, Chen J, Peters LL, Lux SE, Mandel LJ. Distribution of epithelial ankyrin (Ank3) spliceoforms in renal proximal and distal tubules. Am J Physiol. 1998; 274:F129–38. [PubMed: 9458832]

58. Carter PH, Dean T, Bhayana B, Khatri A, Rajur R, Gardella TJ. Actions of the Small Molecule Ligands SW106 and AH-3960 on the Type-1 Parathyroid Hormone Receptor. Mol Endocrinol. 2015; 29:307–21. [PubMed: 25584411]

59. Yang D, Guo J, Divieti P, Bringhurst FR. Parathyroid hormone activates PKC-delta and regulates osteoblastic differentiation via a PLC-independent pathway. Bone. 2006; 38:485–96. [PubMed: 16325485]

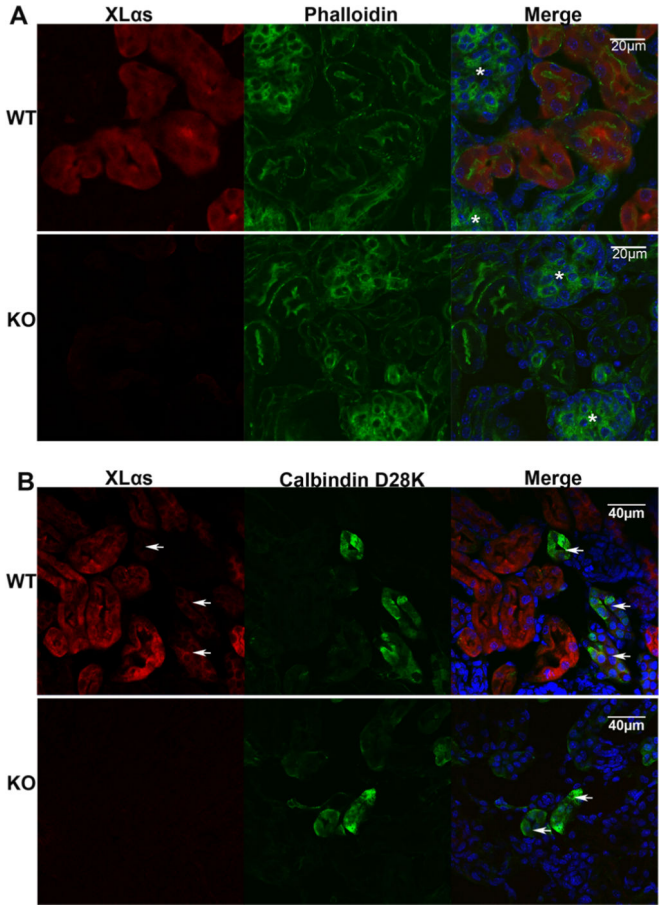

Fig. 1. XLαs is located in renal proximal tubules and distal tubules at early postnatal stages

(**A**) Immunofluorescence staining of XLαs in kidneys taken from P2 wild-type (WT) and XLKO (KO) mice. XLαs is shown in red, phalloidin (to stain F-actin) is in green, and nuclei are in blue. Asterisks indicate glomeruli. Scale bar: 20 μm. (**B**) Immunofluorescence staining of XLαs and the Ca^{2+}-binding protein Calbindin D-28K in kidneys taken from P2 WT and XLKO mice. XLαs is shown in red, Calbindin D-28K is shown in green, and nuclei are in blue. Arrows indicate distal tubules that are positive for Calbindin D-28K staining. Scale bar: 40 μm. Images in all panels are representative of three independent experiments.

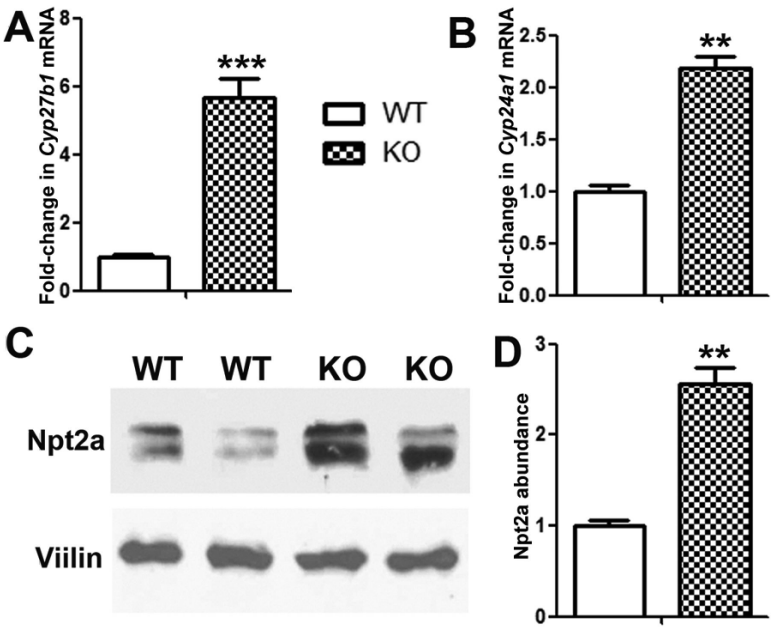

Fig. 2. P2 XLKO mice have increased amounts of *Cyp27b1* and *Cyp24a1* mRNAs and Npt2a protein

(**A** and **B**) Whole kidneys from WT and XLKO mice were processed and then analyzed by qRT-PCR to determine the relative amounts of (A) *Cyp27b1* and (B) *Cyp24a1* mRNAs. Data are means ± SEM of littermates from three independent litters (n = 12 mice per group). $^{**}P < 0.01$, $^{***}P < 0.001$. (**C**) Renal brush-border membranes isolated from WT and XLKO mice were subjected to Western blotting analysis to detect Npt2a protein. Villin was used as a loading control. Western blots are representative of three independent experiments. (**D**) Densitometric analysis of the relative abundance of Npt2a protein normalized to that of villin in WT and XLKO from the experiments represented in (C). Data are means ± SEM of seven mice from each group. $^{**}P < 0.01$.

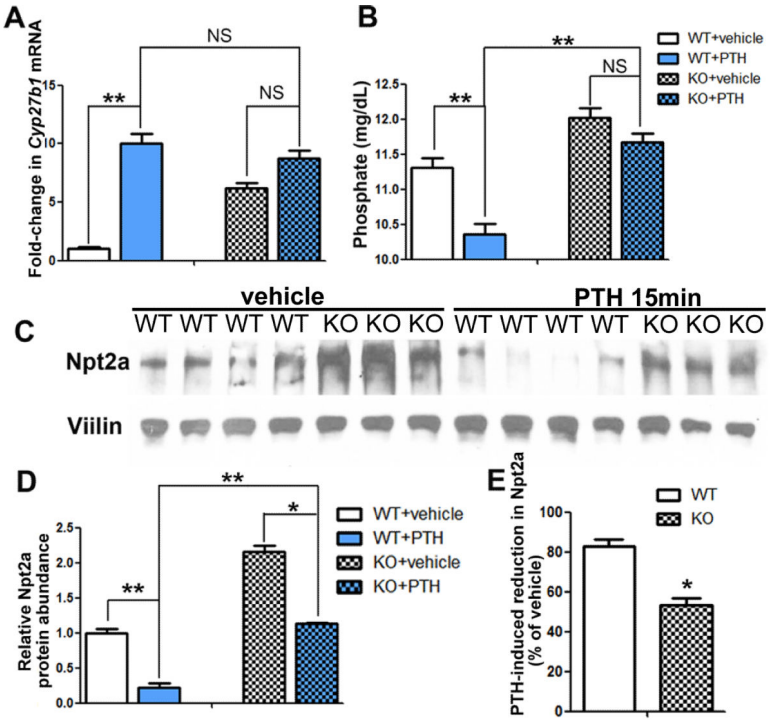

Fig. 3. P2 XLKO mice exhibit resistance to PTH

(**A** and **B**) P2 WT and XLKO littermate mice were injected s.c. with vehicle (10 to 12 mice per group) or PTH (50 nmol/kg, six mice per group). Two hours later, the mice were subjected to (A) qRT-PCR analysis of the relative abundance of *Cyp27b1* mRNA in P2 kidneys and (B) analysis of the serum concentrations of phosphate. Data are means ± SEM of four independent experiments. ***P* < 0.01; NS, not significant. (**C**) P2 WT and XLKO littermate mice were injected s.c. with vehicle or PTH (50 nmol/kg). Fifteen minutes later, renal brush-border membranes were isolated and subjected to Western blotting analysis of Npt2a protein. Villin was used as a loading control. Western blots are representative of four independent experiments. (**D**) Densitometric analysis of the relative abundance of Npt2a protein normalized to that of villin in WT and XLKO mice from the experiments represented in (C). Data are means ± SEM of six or seven mice from each group. **P* < 0.05, ***P* < 0.01. (**E**) Extent of the PTH-induced reduction in Npt2a abundance in the indicated WT and XLKO mice relative to that in vehicle-treated mice. Data are means ± SEM of three independent experiments. **P* < 0.05.

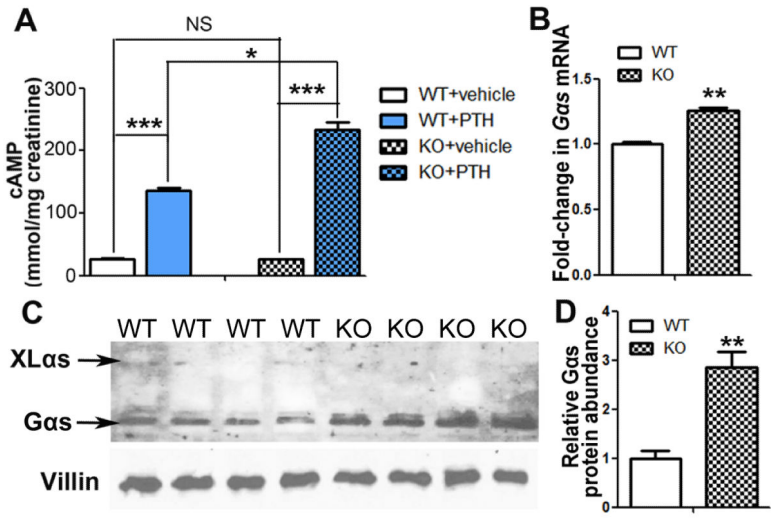

Fig. 4. Gαs abundance in proximal tubules and PTH-induced concentrations of urinary cAMP are increased in P2 XLKO mice

(**A**) P2 XLKO and WT littermate mice were injected s.c. with vehicle or PTH (50 nmol/kg). Fifteen minutes later, the concentrations of cAMP in the urine of the mice were determined and expressed relative to the amounts of urinary creatinine. Data are means ± SEM of six to nine mice per group from three independent experiments. **P* < 0.05; ****P* < 0.001; NS, not significant. (**B**) Whole kidneys from P2 WT and XLKO mice were subjected to qRT-PCR analysis to determine the relative amounts of *Gsα* mRNA. Data are means ± SEM of 12 mice per group from four independent experiments. ***P* < 0.01. (**C**) Renal brush-border membranes isolated from WT and XLKO mice were subjected to Western blotting analysis with an antibody that recognizes both Gαs and XLαs, as indicated. Villin was used a loading control. (**D**) Densitometric analysis of the relative abundance of Gαs protein normalized to that of villin in WT and XLKO mice from the experiments represented in (C). Data are means ± SEM of four mice from each group. ***P* < 0.01.

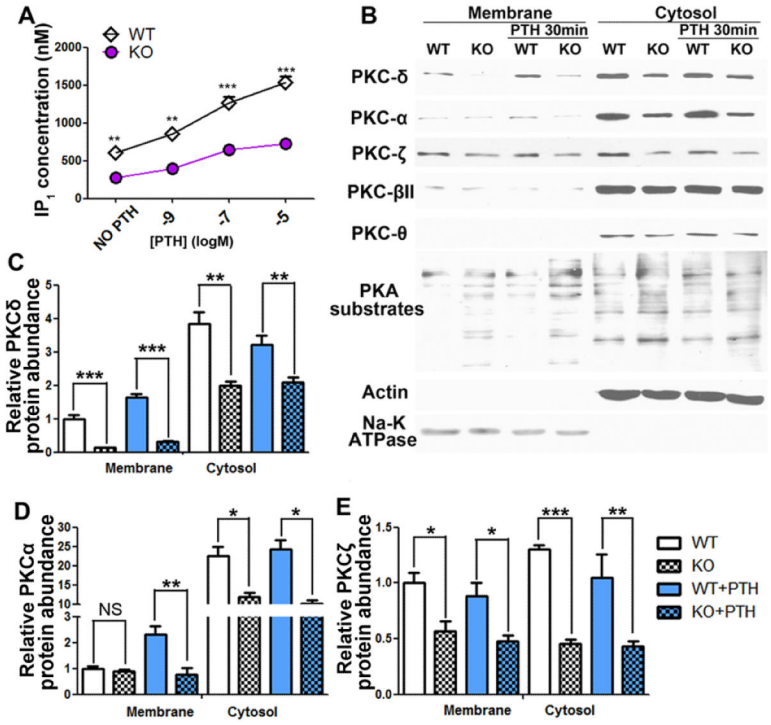

Fig. 5. Basal and PTH-stimulated $G_{q/11}$ signaling is suppressed in P2 XLKO mice

(**A**) Proximal tubule–enriched renal cortices isolated from P2 WT and XLKO littermate mice were left untreated or were treated with the indicated concentrations of PTH for 30 min. IP_1 concentrations were then determined as described in the Materials and Methods. Data are means ± SEM of eight mice per group from two independent experiments. (**B**) Proximal tubule–enriched cortices isolated from P2 WT or XLKO mice were left untreated or were treated with PTH for 30 min. Samples were then subjected to fractionation, and the indicated membrane and cytosolic fractions were subjected to Western blotting analysis with antibodies specific for the indicated proteins. Western blots are representative of three independent experiments that combined samples from four to five pups of each genotype. (**C** to **E**) Densitometric analysis of the relative abundances of (C) PKCδ, (D) PKCα, and (E) PKCζ proteins in the membrane and cytosolic fractions of the indicated mice from the experiments represented in (B). Data are means ± SEM of three independent experiments. **P* < 0.05, ***P* < 0.01, ****P* < 0.001; NS, not significant.

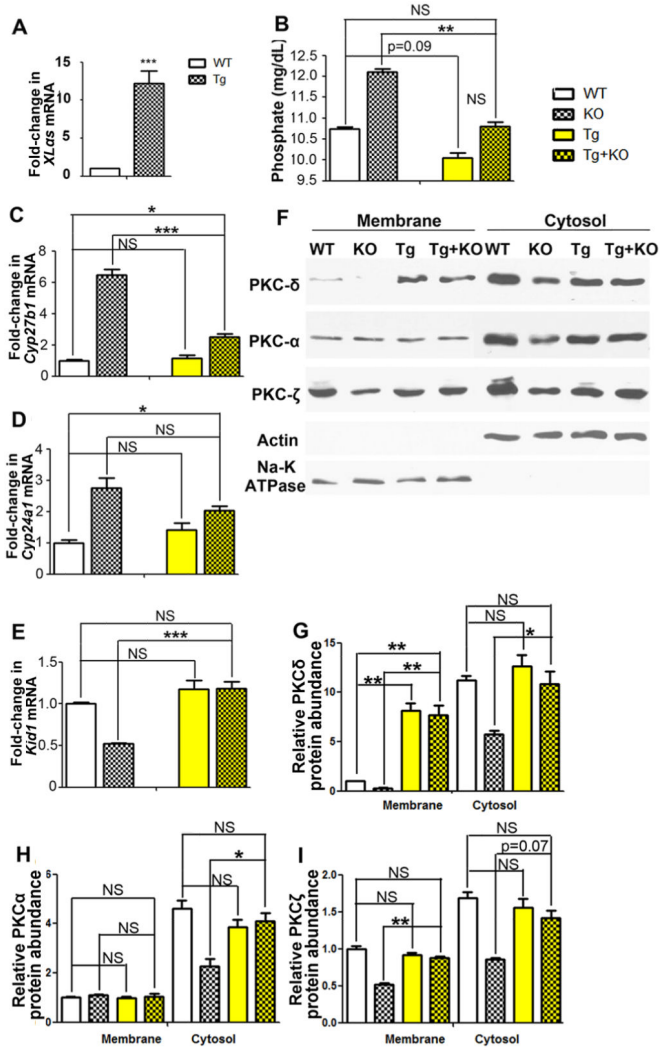

Fig. 6. Transgenic overexpression of XLαs specifically in proximal tubules rescues the phenotype of P2 XLKO mice

(**A**) Whole kidneys from P2 WT and rptXLαs (Tg) littermate mice were analyzed by qRT-PCR to determine the relative abundance of XLαs mRNA. Data are means ± SEM of four independent experiments. (**B**) Serum phosphate concentrations in P2 WT, XLKO, rptXLαs (Tg), and XLKO:rptXLαs (Tg+KO) littermate mice. Data are means ± SEM of 12 to 15 mice per group from seven litters. (**C** to **E**) Kidneys from the indicated P2 littermate mice were subjected to qRT-PCR analysis to determine the relative abundances of (C) *Cyp27b1*, (D) *Cyp24a1*, and (E) *Kid1* mRNAs. Data are means ± SEM of six mice per group from three litters. (**F**) Kidneys from the indicated P2 littermate mice were subjected to subcellular fractionation and Western blotting analysis with antibodies against the indicated proteins. Western blots are representative of three independent experiments. (**G** to **I**) Densitometric analysis of the relative abundances of (G) PKCδ, (H) PKCα, and (I) PKCζ proteins in the membrane and cytosolic fractions of the indicated mice from the experiments represented in (F). Data are means ± SEM of four to five mice per group combined from three independent experiments.

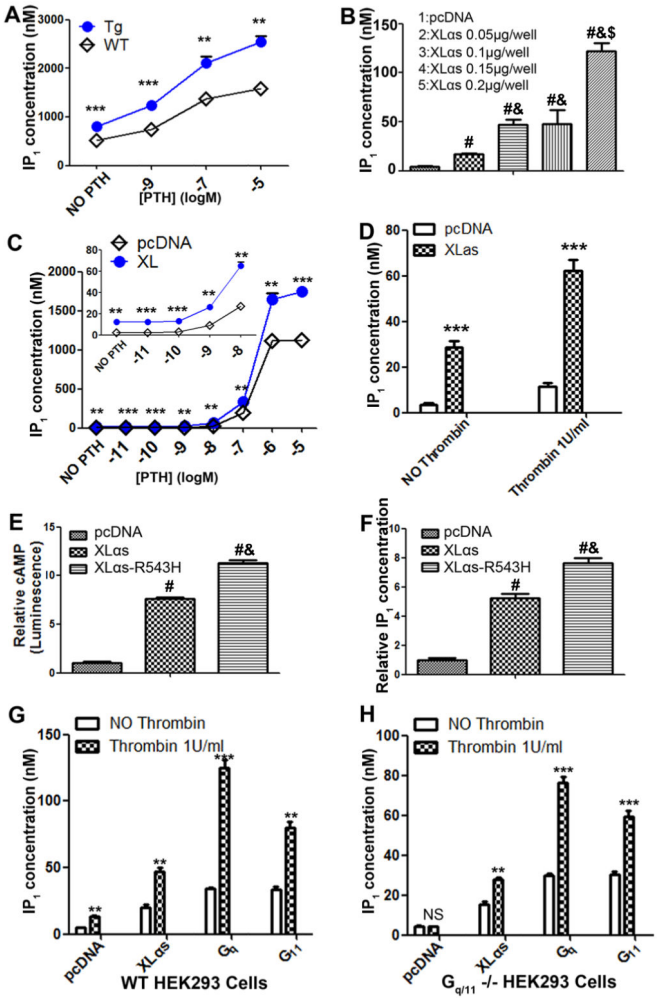

Fig. 7. Overexpression of XLαs induces basal and agonist-stimulated generation of IP_3

(**A**) Proximal tubule–enriched cortices isolated from P2 WT and rptXLαs (Tg) littermate mice were left untreated or were treated with the indicated concentrations of PTH before being analyzed to determine the amounts of IP_1. Data are means ± SEM of eight mice per group from three independent experiments. (**B**) HEK 293 cells transfected with control plasmid (pcDNA) or with increasing concentrations of plasmid encoding XLαs were analyzed to determine their IP_1 concentrations under unstimulated (basal) conditions. Data are means ± SEM of eight experiments. $^{\#}P < 0.05$ between group 1 and group 2; $^{\&}P < 0.05$ between group 2 and groups 3 and 4; $^{\$}P < 0.05$ between group 5 and groups 3 and 4. (**C**) HEK 293 cells stably expressing PTHR were transfected with control plasmid (pcDNA) or with plasmid encoding XLαs and then were left untreated or were treated with the indicated concentrations of PTH for 30 min. Samples were analyzed to determine the amounts of IP_1. Data are means ± SEM of eight samples per group from four experiments. Inset: The same data presented with a different y-axis scale for the lower concentrations of PTH. (**D**) HEK 293 cells transfected with control plasmid or plasmid encoding XLαs were left untreated or were treated with thrombin (1 U/ml) for 30 min before being subjected to IP_1 analysis. Data are means ± SEM of eight samples per group from four experiments. (**E** and **F**) HEK 293

cells transfected with control plasmid or with plasmids encoding WT XLαs or the XLαs-R543H mutant were analyzed to determine the relative amounts of (E) cAMP and (F) IP_1 under basal conditions. Data are means ± SEM of 12 samples per group from four independent experiments. $^{\#}P < 0.05$ when comparing between pcDNA-transfected cells and cells expressing WT XLαs; $^{\&}P < 0.05$ when comparing between cells expressing WT XLαs and cells expressing XLαs-R543H. (**G** and **H**) WT HEK 293 cells (G) and $G_{q/11}^{-/-}$ HEK 293 cells (H) were transiently transfected with control plasmid (pcDNA) or with plasmids encoding XLαs, G_q, or G_{11}, as indicated. The cells were then left unstimulated or were stimulated with thrombin (1 U/ml) for 30 min before being analyzed to determine their amounts of IP_1. Data are means ± SEM of 12 samples per group from four independent experiments. $^{**}P < 0.01$, $^{***}P < 0.001$; NS, not significant.

Table 1

Comparison of serum biochemistries.

	WT	XLKO
Phosphate (mg/dl)	10.32 ± 0.24	11.42 ± 0.41*
Ca^{2+} (mmol/l)	1.48 ± 0.01	1.42 ± 0.02*
PTH (pg/ml)	65.25 ± 1.34	138.10 ± 4.99*
$1,25(OH)_2D$ (pmol/l)	183.42 ± 4.64	378.02 ± 6.86***
FGF23 (pg/ml)	524.11 ± 11.64	158.86 ± 9.29***

**$P < 0.01$

Analysis of the serum concentrations of phosphate, Ca^{2+}, PTH, $1,25(OH)_2D$, and FGF23 in P2 WT and XLKO mice. Data are means ± SEM of 18 to 27 (WT) or 14 to 20 (XLKO) mice combined from four to seven litters.

*$P < 0.05$

***$P < 0.001$.